buildings

MDPI

Article

Synergistic Effect of Combined Polymorphs Anatase-Rutile Nano-Modified Lightweight Concrete on Photocatalytic Reduction of NO_x, Self-Cleaning Performance, and Antimicrobial Properties

Weronika Kujawa [1,2,*], Agnieszka Didyk-Mucha [2], Ewa Olewnik-Kruszkowska [1,*], Magdalena Gierszewska [1] and Anna Rudawska [3]

[1] Department of Physical Chemistry and Physicochemistry of Polymers, Faculty of Chemistry, Nicolaus Copernicus University in Toruń, Gagarin 7 Street, 87-200 Toruń, Poland; mgd@umk.pl
[2] Selena Industrial Technologies sp. z o.o., Pieszycka 1 Street, 58-200 Dzierżoniów, Poland; agnieszka.didyk@selena.com
[3] Department of Production Engineering, Faculty of Mechanical Engineering, Lublin University of Technology, 20-618 Lublin, Poland; a.rudawska@pollub.pl
* Correspondence: weronika.kujawa@doktorant.umk.pl (W.K.); olewnik@umk.pl (E.O.-K.); Tel.: +48-532-720-966 (W.K.); +48-56-611-2210 (E.O.-K.)

Abstract: Anatase, one of the polymorphs of titanium dioxide (TiO_2), has become the most widely used semiconductor for photocatalytic materials due to its chemical and physical properties. However, researchers have been studying the use of alternative materials (e.g., ZnO, N-doped, and C-doped TiO_2) to improve the photocatalytic activity of cementitious materials. In this paper, we propose a modification of lightweight concrete by introducing mixed phases of titanium dioxide—anatase and rutile—to enhance its photocatalytic performance. The efficiency of NO_x degradation of nano TiO_2-modified concrete, its self-cleaning performance, and its antimicrobial properties were studied. The photocatalytic activity of lightweight concrete without TiO_2 and concrete with the addition of anatase, rutile, and anatase-rutile was compared. The results show that modifying the samples by adding a mixture of anatase and rutile (2.5 wt % A + 2.5 wt % R) significantly improved the photocatalytic performance of lightweight concrete.

Keywords: photocatalyst; titanium dioxide; lightweight concrete; reduction of NO_x; self-cleaning performance; antimicrobial properties

check for updates

Citation: Kujawa, W.; Didyk-Mucha, A.; Olewnik-Kruszkowska, E.; Gierszewska, M.; Rudawska, A. Synergistic Effect of Combined Polymorphs Anatase-Rutile Nano-Modified Lightweight Concrete on Photocatalytic Reduction of NO_x, Self-Cleaning Performance, and Antimicrobial Properties. *Buildings* **2023**, *13*, 1736. https://doi.org/10.3390/buildings13071736

Academic Editors: Daniel Wałach and Piotr Dybeł

Received: 5 June 2023
Revised: 25 June 2023
Accepted: 4 July 2023
Published: 8 July 2023

Copyright: © 2023 by the authors. Licensee MDPI, Basel, Switzerland. This article is an open access article distributed under the terms and conditions of the Creative Commons Attribution (CC BY) license (https://creativecommons.org/licenses/by/4.0/).

1. Introduction

Lightweight concrete is widely used in building construction, especially as the main element of external facade systems [1,2]. Therefore, lightweight concrete structures are routinely exposed to different environmental conditions such as humidity, temperature, air pollutants, and microbes. The visual contamination of concrete by microorganisms and air pollutants is a common problem with existing buildings [3–7]. The consequences of microbial adhesion to the surface of concrete walls and their colonization by microorganisms are mainly aesthetic. Still, they can also cause the deterioration of the concrete in the most extreme cases, leading to an increase in the cost of repair or replacement [7–9]. One of the possible ways to prevent these issues is the application of nano-modified cementitious materials in construction.

A literature review indicates various options for improving the performance and changing the concrete parameters with the use of nanotechnology [10–15]. The most widely used and fully tested nanomaterials added into cement-based composites include nano-silica [16,17], nano-alumina [18], and nano-clay [19], which promote and accelerate the pozzolanic chemical reaction, imparting increased mechanical strength to the concrete.

Other nanomaterials that can be employed to reinforce concrete are graphite [20] and carbon nanotubes [21]. Moreover, the nanocomponents can act as a filler, leading to a reduction in the porosities of concrete and an increase in the packing density [22]. The introduction of nanomaterials to the cementitious matrix also imparts special properties to the concrete, such as photocatalytic properties [23,24], antimicrobial properties [6], self-cleaning performance [25], thermal insulation [17], and electrical conductivity [26]. Based on this knowledge, introducing nanoparticles into the cementitious matrix can lead to the formation of new materials and could be a part of the concept in developing new, smart buildings in the future.

Over the last few years, many materials that show photocatalytic properties have been studied [13,27]. These materials include titanium dioxide (TiO_2), cadmium sulfide (CdS), zinc oxide (ZnO), and more advanced chemical compounds, including oxides infused with other metals [13,28,29]. The most widely recognized photocatalyst comprises nanometric titanium dioxide, which exists as two main polymorphs—anatase and rutile. The presence of one or both of these phases influences the photocatalytic performance of the material [30]. The third crystal structure of TiO_2—brookite—is highly unstable, making it difficult to prepare, maintain, and apply for practical use [31]. The photocatalytic properties of TiO_2-based cement composites have been studied in many works to determine whether air-purifying [24,32–35], antimicrobial [7], and self-cleaning properties can be obtained [12,36–38], and to determine the impact of those photocatalytic properties on the mechanical and physicochemical characteristics of these composites [25,39–43]. Moreover, it should be stressed that cement-based materials filled with nanometric titanium dioxide have achieved excellent levels of efficiency in terms of NO_x degradation [24,32,33,44]. An insignificant number of studies have been focused on the removal of volatile organic compounds (VOC) by cementitious materials that have been produced with the addition of nanometric titanium dioxides, such as acetaldehyde [34] and toluene [35]. The introduction of TiO_2 into cementitious composite causes significant improvement in its self-cleaning performance compared to that of the same material without a photocatalyst [38,45,46]. It should be emphasized that the potential of photocatalytic concrete to inhibit the growth of bacteria [47,48], algae [49], and fungi [50] on its surface has also been proved [38,45,46]. Janus et al. found that the presence of 10 wt % of TiO_2-based photocatalyst in concrete improved its antibacterial properties under visible light irradiation, and a total impediment of *E. coli* was observed [51]. Moreover, the authors indicated that the incorporation of nitrogen into the structure of the photocatalyst contributed to the enhancement of the antibacterial properties of the concrete. A similar effect in terms of inhibiting *E. coli* growth was observed by Ganji et al. [52], who indicated that the addition of 5 wt % TiO_2 was optimal in their cement samples. Fonseca et al. [53] proposed the utilization of anatase for preventing the biodeterioration of mortar caused by cyanobacteria and chlorophyta, which demonstrated better efficiency than conventional biocides. The research conducted by Clovis et al. [54] showed that the attachment and growth of *Oedogonium* algae were inhibited by a TiO_2-based cement coating. Tuntachon et al. [55] investigated the resistance to fungi and algae formation on the surface of a geopolymer containing nano-titanium dioxide. The results showed that an increase in the addition of nano-titanium dioxide by up to 5 wt % increases the mixture's ability to resist fungi and algae growth on the sample's surface. Furthermore, the enhanced biodeterioration and biofouling resistance seen in concrete with the addition of combined nano-TiO_2 and nano-$CaCO_3$ was observed in studies conducted by Harilal et al. [56]. In the case of lightweight concrete, which can be applied as a facade material, it is crucial to prevent the occurrence of biofouling by microorganisms due to the risk of material biodegradation. Hence, it is imperative to conduct studies on the antimicrobial properties of lightweight concrete. Photocatalysis can be described as a chemical process requiring a semiconductor that absorbs photons and further induces electron-hole pairs in valence and conduction bands [31]. The migration of the electron holes to the surface of materials reduces the chemical potential. At the same time, the semiconductor continues to degrade the molecules adsorbed onto the surface

of the material [57,58]. The efficiency of the photocatalyst influences both the material and the environmental factors. The results of a previous study [59] showed that the most important factors influencing photoactivity include the type of photocatalyst used, its quantity, and the application method (i.e., coating). Environmental factors include UV radiation intensity, wind speed, ambient temperature, and relative humidity. The ideal conditions for activating the photocatalysis process are sunny days with a low wind speed and temperatures above 25 °C.

It should be noted that in natural sunlight, anatase, the most commonly used photocatalyst, is capable of degrading NO_x, due to redox processes occurring on the catalyst's surface (Figure 1) [60].

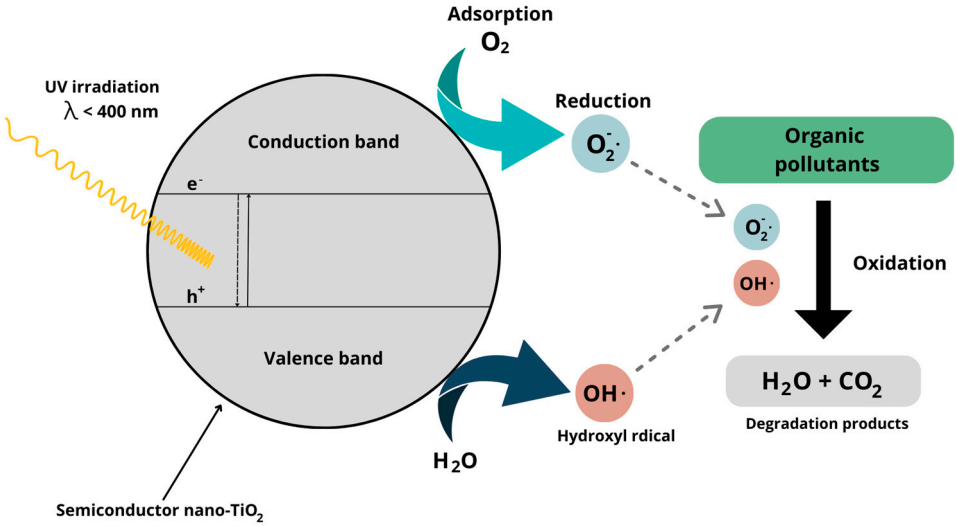


Figure 1. Scheme of the photo-catalytic process in the nano-TiO_2 particles (based on [61]).

Generally, photocatalysis begins as a result of the oxidation of NO_x by the hydroxyl radical $^{\bullet}OH$ and superoxide radical $O_2^{\bullet-}$, which leads to the formation of nitrite NO_2^- and/or nitrate NO_3^- via a series of reactions that occur according to the following patterns [33]:

$$TiO_2 \overset{hv}{\rightarrow} TiO_2 + e^- + h^+ \quad (1)$$

$$h^+ + H_2O \rightarrow H^+ + OH^{\cdot} \quad (2)$$

$$e^- + O_2 \rightarrow O_2^{\cdot -} \quad (3)$$

$$NO + O_2^{\cdot -} \rightarrow NO_3^- \quad (4)$$

$$NO + OH^{\cdot} \rightarrow NO_2 + H^+ \quad (5)$$

$$NO + OH^{\cdot} \rightarrow HNO_2 \quad (6)$$

$$HNO_2 + OH^{\cdot} \rightarrow NO_2 + H_2O \quad (7)$$

$$NO_2 + OH^{\cdot} \rightarrow NO_3^- + H^+ \quad (8)$$

The products of reactions (4) and (8) (nitrate ions) are water-soluble and are washed away from the active surface by rainfall [62,63].

Considering the external surface exposure of the lightweight concrete, its large surface area as a building façade, and the promising previous results of TiO_2-based cement composites, it seems to be an interesting further development of the material to create self-cleaning, antimicrobial, and pollution-removing cementitious materials for external application use in built-up areas. In the literature, however, no research work has been devoted to describing the potential photocatalytic properties of cementitious materials using rutile or a combination of rutile and anatase as a photocatalyst. In this work, pho-

tocatalytically modified lightweight concrete mixed with different polymorphs of TiO_2 was prepared and tested. The main objective of this research is to compare the results of the addition of anatase, rutile, and a mixture of rutile and anatase to lightweight concrete, and their effect on the reduction of nitrogen oxides (NO_x), self-cleaning performance, and prevention of the growth of fungi and algae on its surface.

2. Materials and Methods

2.1. Materials

The compounds used in advanced construction chemicals were obtained from local producers and distributors. A mixture of fillers consisting of 0.1–0.5 mm sand from ZWP MOSTY Sp. z.o.o. (Chęciny, Poland), limestone from Czatkowice (Krzeszowice, Poland), and lightweight perlite from IMCD (Rotterdam, The Netherlands) were used. The properties of the indicated aggregates are detailed in Table 1. Ordinary Portland cement (OPC) 52,5 R-NA was obtained from "Cemex" (Rudniki, Poland), metakaolin from IMCD (Rotterdam, The Netherlands), and calcium aluminate from IMCD (Rotterdam, The Netherlands) were used as a binder system. Moreover, the following chemical additives were used: Melflux 2651F—a polycarboxylate-based superplasticizer, provided by the BASF company (Ludwigshafen, Germany); tartaric acid, which is a commonly used retarder for Portland cement, obtained from CFI World (Robakowo, Poland); hydroxyethyl cellulose (HEC), also named Tylose H300P2, provided by SE Tylose (Wiesbaden, Germany); redispersible polymer powder (RDP) Vinnapas 4410L (Wacker Chemie, Burghausen, Germany); the defoamer Agitan P84 9 (Münzing Chemie, Heilbronn Germany). Two different polymorphous phases of titanium dioxide—anatase (A) and N- doped rutile (R)—were both provided by Cinkarna (Celje, Slovakia). The parameters of the titanium dioxide used in the study are listed in Table 2.

Table 1. Parameters of the aggregates used.

Aggregate Properties	Size (mm)	Water Absorption (%)	Specific Gravity (g/dm^3)
Sand	0.1–0.5	<0.1	1550
Limestone	<0.1	<2.0	900–1100
Perlite	<0.1	<0.1	115

Table 2. Parameters of the titanium dioxide used in the research.

Characteristics	Anatase	Rutile
Density	1.2 g/cm^3	1.2 g/cm^3
Crystal size (Scherrer)	10 nm	30 nm
Specific surface area	250 m^2/g	60 m^2/g

2.2. Sample Preparation

Lightweight concrete without nanometric titanium dioxide was used as a control, and 9 nanophase-modified lightweight concrete specimens were produced at a water/cement (w/c) ratio of 0.24. The prepared materials consisted of 580 g of ordinary Portland cement, 56 g of metakaolin, 50 g of calcium aluminate, 1126 g of sand, 200 g of limestone, 100 g of perlite, 10 g of superplasticizer, 30 g of re-dispersible polymer powder, 2.6 g of hydroxyethyl cellulose, and 2 g of antifoam. Different forms of titanium dioxide were incorporated into the dry mixture, with designated contents of 1 wt %, 2.5 wt %, and 5 wt %. The compositions of the obtained samples are presented in Figure 2.

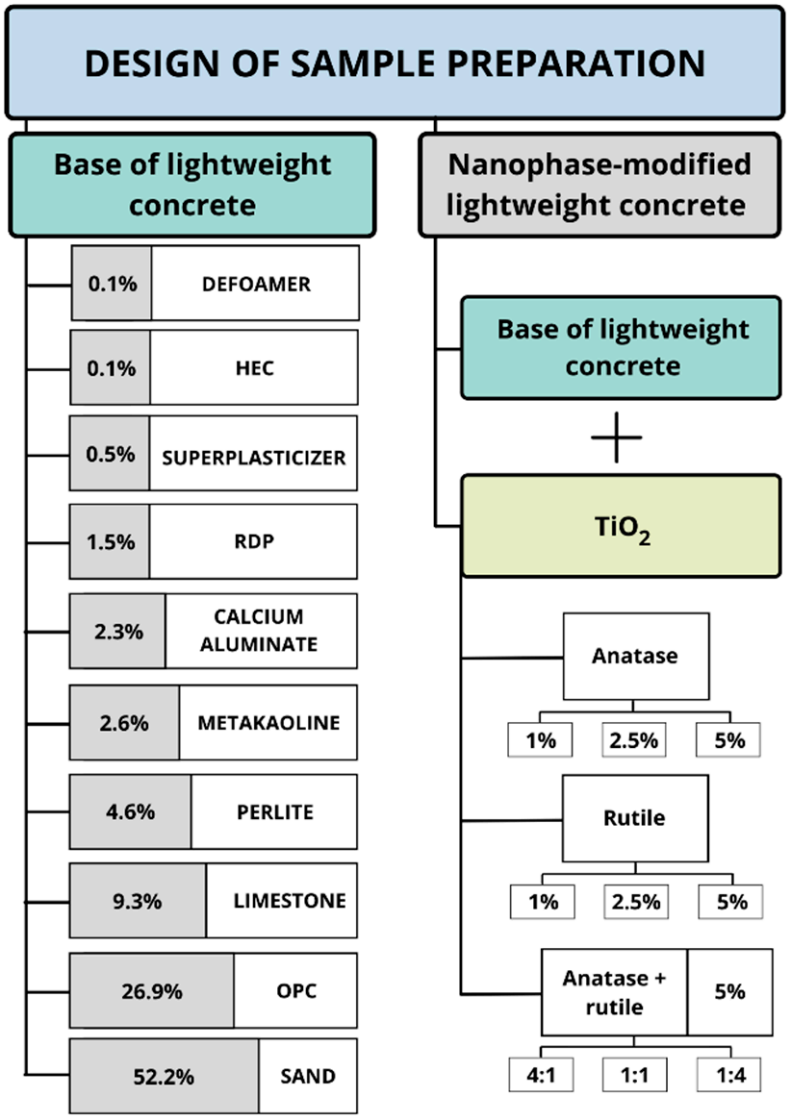


Figure 2. Composition of the obtained samples.

The samples were prepared in a mixer in accordance with the requirements of the EN 196-1:2016 standard [64]. The dry materials, including binders, fillers, and chemical additives, were mixed to ensure the homogenization of ingredients. Afterward, the dry part of the mixture was added into the bowl of the mixer with a specified amount of water and mixed for 2 min. After 5 min, the fresh concrete was re-mixed for 1 min. The concrete samples were formed as 160 mm × 40 mm × 40 mm cuboids in metal molds. The covered molds were placed in a cabinet with 90% relative humidity and a temperature of 20 ± 1 °C. Samples were extracted from the molds after 24 h and were then placed in an airy room with 65 ± 5% relative humidity and stored at 23 ± 2 °C for 27 days.

2.3. Photocatalytic Conversion of NO_x

The degradation of NO_x compounds when employed in cement–polymer concrete with nano-TiO_2 was studied experimentally. The experiments were carried out in a photoreactor, which was designed according to an applicable ISO 22197-1 standard [65] to assess the type of photocatalytic concrete, employing NO as the pollutant source. The NO inlet concentration and flow rate during this study were 3 dm^3/min. The apparatus comprised a reactor cell, a light source, a gas supply, and a NO_x analyzer (Figure 3). The intensity of the UV-A light was 1 mW/cm^2.

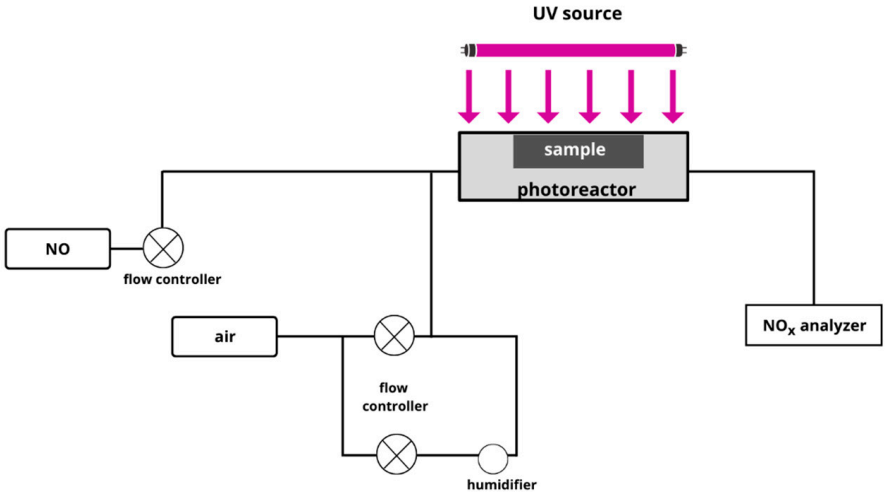


Figure 3. Scheme of the photocatalytic reaction test for NO_x degradation.

2.4. Self-Cleaning Performance

The self-cleaning capacity of the samples was studied based on the de-coloration of an organic dye—rhodamine B—which is commonly used for tests on different building materials. Rhodamine solution was deposited onto the surface of the analyzed panels. After impregnation, the samples were stored in the dark for 24 h, then the color intensity value of the samples was measured using a spectrophotometer (X-RITE VS 450, Grand Rapids, MI, USA). Additional measurements were carried out after 48 h and after 7 days of irradiation. The degree of de-coloration was calculated according to Equation (9):

$$\% \text{ of color change } = \frac{a_0 - a_t}{a_0} \quad (9)$$

where a_0 represents the color intensity value before the exposure and a_t represents the values obtained after irradiation.

2.5. Antimicrobial Properties

The microbial test method was applied to assess the lightweight concrete's susceptibility to fungal and algae proliferation. The method determines the level of surface protection and the effectiveness of titanium dioxide being introduced in various concentrations into samples of lightweight concrete and modified with a nanophase. The experiments were carried out according to the internal test methods D. 850-2 and D.800.2, classified by the Thor GmbH Company (Speyer, Germany). Green algae (*Stichococcus bacillaris* and *Scenedesmus vacuolatus)* and fungi (*Aspergillus niger* and *Penicillium funiculosum)* were selected because they naturally populate concrete surfaces. The fungal inoculum contained 10^6 cells/mL, whereas the algal inoculum contained 10^5 cells/mL. The samples intended for testing were prepared in two groups—without water irrigation or stored for two days in water before the experiment—in standard conditions. In the next stage, samples of the inoculum were placed on Petri dishes in an agar medium and were then sprayed with 10^6 cells/mL of fungi or 10^5 cells/mL of algae. Subsequently, the samples were stored to evaluate fungal/algal growth using a comparative scale that is presented in Tables 3 and 4. The scheme of the test stages is shown in Figure 4.

Table 3. The grading scale for the surface growth of the fungi.

Scale	Surface Growth of the Fungi
0	No fungal growth on the surface of the sample. Free zone of fungal growth around the sample.
(0)	No fungal growth on the surface of the sample or trace amounts of fungus at the edges of the sample. No free zone of fungal growth around the sample.
1	Fungal growth over less than 25% of the tested surface.
2	Fungal growth over between 25 and 50% of the tested surface.
3	Fungal growth over more than 50% of the tested surface.

Table 4. The grading scale for the surface growth of the algae.

Scale	Surface Growth of Algae
0	No surface growth of algae or a trace amount of algae.
1	Poor algal growth over less than 25% of the tested surface.
2	Moderate algal growth over between 25 and 50% of the tested surface.
3	Strong algal growth over more than 50% of the tested surface.

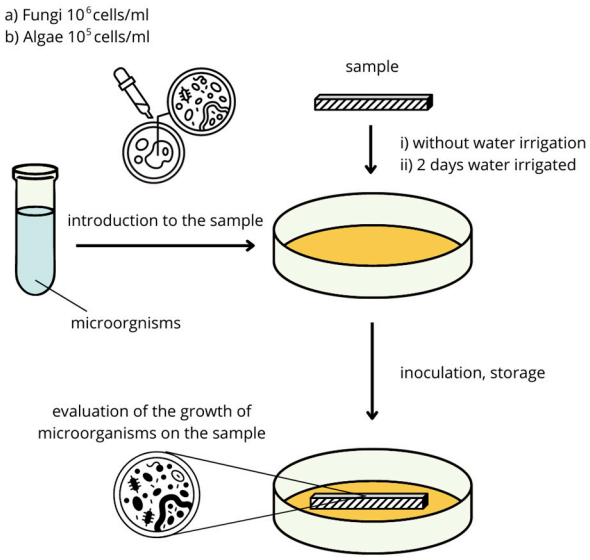


Figure 4. The scheme of the test stages.

3. Results and Discussion

3.1. Antimicrobial Properties

The formation of biofouling is a significant problem for the construction industry. Walls and facades are regularly affected by bacteria and algal and fungal growth, causing material biodegradation [6]. Fungi can produce certain pigments and biogenic acids, leading to concrete damage as a result of the formation of insoluble calcium complexes. Moreover, they are able to penetrate the concrete surface. These processes promote material weight loss and increase the permeability and porosity of concrete [7,66]. In order to inhibit biofouling, it is crucial to stop the growth of algae and fungi cells during the first step of biofilm formation, when only reversible attachment created by non-specific forces occurs. Irreversible binding, in which the extracellular polymer forms a thick outer layer (the second stage of biofilm formation) to protect the microorganisms from damage, must be prevented [67,68]. One of the methods of preventing the formation of irreversible biofilm, which is very difficult to remove, is the rapid removal of organic pollutants (which are an

excellent growth medium for microorganisms) from the surface [67]. Cementitious coatings containing photocatalytic titanium dioxide may help in this endeavor [7,69].

Since Matsunaga et al. [70] first demonstrated the photocatalytically powered antimicrobial properties of TiO_2, many articles have discussed the bactericidal mechanisms of TiO_2 [69]. As mentioned earlier, there are no publications describing the potential photocatalytic properties of cementitious materials that incorporate rutile and a combination of rutile and anatase as a photocatalyst.

In this paper, to determine the level of surface protection, the antimicrobial properties of TiO_2 nanophase-modified lightweight concrete were tested. The effect of titanium dioxide concentrations and the ratio of anatase-rutile polymorphs on the susceptibility to the fungal and algal proliferation of photocatalytically modified lightweight concrete was also investigated. To establish the antimicrobial activity of TiO_2 when introduced to lightweight concrete, the fungal and algal strains were inoculated onto cementitious samples, either onto a sample containing TiO_2 or onto a control sample without TiO_2. The test results are shown in Table 5. The grading scales of the fungi and algae surface growth are presented in Tables 3 and 4, respectively.

Table 5. Fungicidal and algicidal film preservation.

Sample	Fungal Growth		Algal Growth	
	I	**II**	**I**	**II**
Control	(0)	3	0	3
1 wt % Anatase	(0)	2	0	3
2.5 wt % Anatase	(0)	1	0	3
5 wt % Anatase	(0)	(0)	1	3
1 wt % Rutile	(0)	1	0	2
2.5 wt % Rutile	(0)	2	0	2
5 wt % Rutile	(0)	3	0	1
4 wt % Anatase + 1 wt % Rutile	(0)	1	0	2
2.5 wt % Anatase + 2.5 wt % Rutile	(0)	(0)	0	2
1 wt % Anatase + 5 wt % Rutile	(0)	1	1	2

I—without water irrigation. II—conditioned for two days in water before the experiment.

The obtained results indicate that there was no significant growth of fungi and algae on the surfaces of all the cement samples (including the control sample without TiO_2) that had not been immersed in water. Water pretreatment caused strong microorganism growth (level 3) on the surface of the control sample, as well as different levels of growth on the TiO_2-modified lightweight concrete surfaces (levels 0–3). This phenomenon can be explained by changes in the physical parameters of concrete after water immersion. Fresh concrete is characterized by a high pH, predominantly pH > 12, which provides natural protection against the biocorrosion caused by the growth of microorganisms, including algae [8]. Over time, the concrete surface becomes inert due to carbonation, the natural aging of the mineral raw materials, and the erosive effect of water. Moreover, water leaching, surface contamination, and immersion in water can increase the roughness of the surface of concrete [71]. This process results in the formation of cavities, where microorganisms can develop. When the pH drops to neutral, favorable conditions are created for the development of heterotrophic factors such as filamentous fungi and algae [9,72]. With a low pH, the control samples in this study lost their natural antimicrobial properties. The modified samples of concrete retained their antimicrobial properties to varying degrees, due to the photocatalytic properties of TiO_2.

The experimental results clearly show the differences in the antimicrobial properties of concrete samples with the addition of both anatase and rutile after exposure to water. This is probably because the antibacterial potential of TiO_2 depends on the ratio of anatase to rutile, due to the variability in photocatalytic activity between these two phases [51].

Increasing the concentration of anatase from 0 wt % to 5 wt % in the TiO_2-modified concrete samples increased the inhibition of biofouling by fungi from level 3 to level 0 (no growth). These results correspond to those reported in the study conducted by Tuntachon et al. [55]. However, this change does not significantly affect the growth of algae—contamination remained at level 3 for all concentrations of anatase. In the case of rutile, the inverse correlation was observed. Increasing the concentration of the mentioned TiO_2 phase caused a decrease in algae biofouling from level 3 to level 1 (weak growth). Taking into account the obtained results, it should be noted that another trend was clearly observed: anatase has a stronger effect on fungi than rutile and is less effective in the case of algae, while in the case of rutile, the opposite effect can be observed. An increase in the concentration of rutile along with a simultaneous increase in the degree of fungal biofouling on the surface of samples was unexpected. In studies conducted by Markowska-Szczupak et al. [73], it was determined that the properties of titanium dioxide are crucial for its antifungal activity. Furthermore, it was observed that differences in fungal structure also had an impact on the final concrete's antifungal properties. The growth of the *P. boydii* and *A. versicolor* strains was strongly inhibited by the presence of titanium dioxide and light, while the growth of the *S. chartarum* strain was stimulated by the presence of titanium dioxide. Additionally, it was indicated that different fungi have different requirements for water and nutrients, which means that adsorbed water and certain impurities (e.g., F-, Na+, and HOO-) on the sample's surface can either inhibit or promote their growth. Considering the aforementioned findings, future detailed research is required.

However, the results clearly show that anatase has better biocidal properties (for fungi and algae) than rutile at the same concentrations. For example, after the introduction of 5 wt % of anatase into a cementitious matrix, level-0 growth can be seen, while for fungi at 5 wt % of rutile, the level-1 growth of algae is observed. Possible explanations for the results described above are the differences in crystallite size, phase structure, specific surface zones, and pore structure [74] of the two mentioned TiO_2 phases. Research shows that anatase has higher photocatalytic activity than rutile because of its better surface adsorption capacity, larger specific surface areas, and smaller particle size [68]. As indicated before, the pretreatment of samples with water can influence the concrete's surface properties. Moreover, better photocatalytic activity facilitates better self-cleaning properties and the possible antimicrobial resistance of TiO_2-modified concrete [69].

It is certainly not without significance that algae can be more difficult to control and may require the presence of higher TiO_2 concentrations. In general, the reactive oxygen species—(ROS) (especially OH radicals), which are photo-generated during electron photoexcitation from the TiO_2 valence band to the conduction band—are responsible for its antimicrobial properties [69]. Moreover, the direct contact of microbial cells with nano TiO_2 also occurs as a result of cell wall damage and cell membrane lipid peroxidation [75]. Basically, the microbial killing process starts from the cell wall and proceeds toward the intracellular components of the cell [51], but it follows a different course for algae and fungi, due to differences in the structure of these two groups of organisms.

In the case of fungi, the denaturation of the fungal cell wall is most important during its disinfection. ROS with high oxidizing power must pass through the rigid fungal cell wall. Photo-generated hydroxyl radicals from TiO_2 are applied to the fungal cell wall surface and directly interact with its glucan and chitin layers (see Figure 5 as a result [75]. In case of algae, ROS also have negative impact on cell wall. Additionally, free radicals directly destroy the chlorophyll molecule resulting in decreasing of photosynthesis efficiency (see Figure 6). Algae may be more resistant to photocatalysis due to possessing more complex and thicker cell walls, extracellular polysaccharide production (which forms a barrier between the cell wall and the photocatalytic surface), and defense mechanisms against ROS evolution [6].

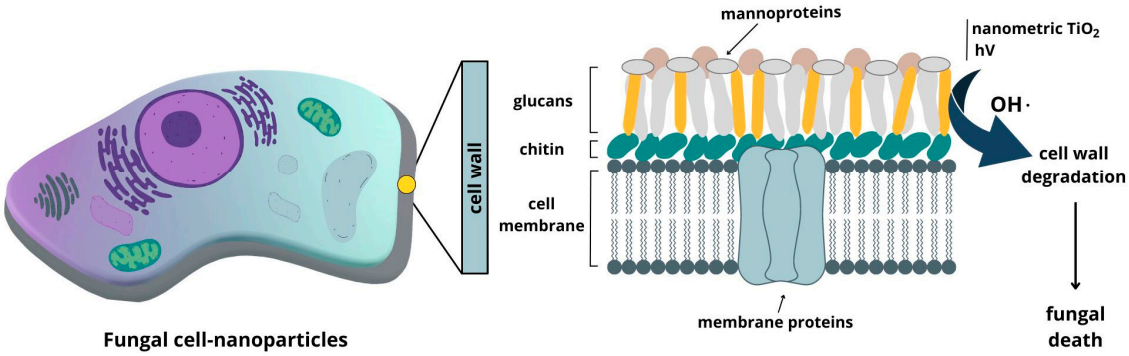


Figure 5. The scheme of fungal cell wall degradation by TiO_2 nanoparticles (based on [76]).

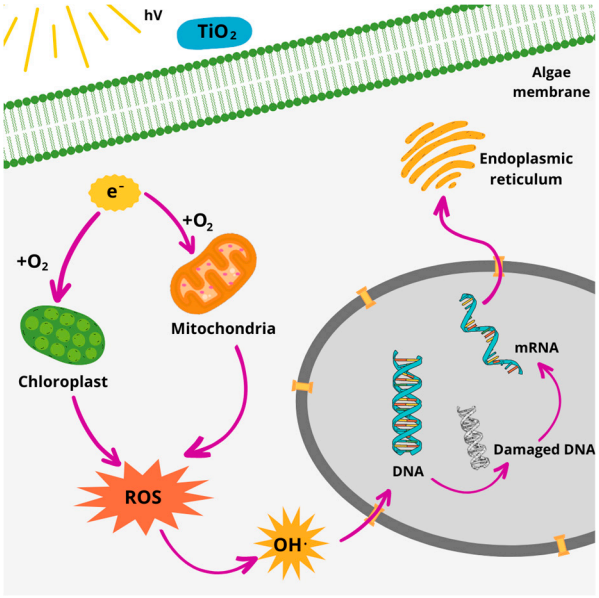


Figure 6. Schematic diagram of the process of the nanometric titanium dioxide, destructively affecting an algae cell (based on [75]).

Interesting interactions have been observed in the case of polymorphic (mixed phase) TiO_2. The research results clearly indicate that the best antifungal and anti-algal properties were simultaneously obtained for the rutile and anatase equilibrium mixture (2.5 wt %). This observation was made in relation to an aqueous suspension of rutile-anatase composite. Krumdieck et al. [77] reported that the rutile-anatase heterojunctions showed higher photocatalytic activity than the single-phase materials separately. Moreover, a similar correlation was recorded to that observed previously when analyzing the anatase and rutile phases separately. Again, the greater effectiveness of anatase against fungi and of rutile against algae was noted.

The synergy between the two phases is poorly understood but yielded promising results. It is worth acquainting oneself with the results of the studies conducted by Jing Hou et al. [75], who noted that the most toxic effect of nano-TiO_2 against algae strongly depended on TiO_2 concentration and exposure time. Further experiments in which the concentration of both anatase and rutile are increased to at least 5 wt % should be carried out. It is very likely that this mixture will achieve a no-growth effect for algae and fungi.

3.2. Self-Cleaning Performance

Many studies [37,46,78–81] have described the self-cleaning performance and photocatalytic activity of cementitious materials that have been modified with nano titanium dioxide. Most results indicate that the addition of 3–5 wt % of nano-TiO_2 to cementitious

materials elicits satisfactory photocatalytic performance. For this reason, samples with different concentrations of TiO_2 were prepared to determine the optimal content of a single phase of rutile and anatase in a tested light cementitious system. Moreover, a 5 wt % ratio of TiO_2 was chosen for the mixed phases.

This work assessed the self-cleaning properties of lightweight concrete that had been modified with TiO2 nanophase, using a colorimetric analysis of the level of discoloration from an organic dye—rhodamine B—the molecules of which are destroyed in the photodegradation process.

The influence of titanium dioxide concentrations and the ratio of anatase-rutile polymorphs of the prepared samples on self-cleaning performance was determined. The samples were prepared in accordance with the scheme presented in Figure 2. The test results are shown in Figure 7.

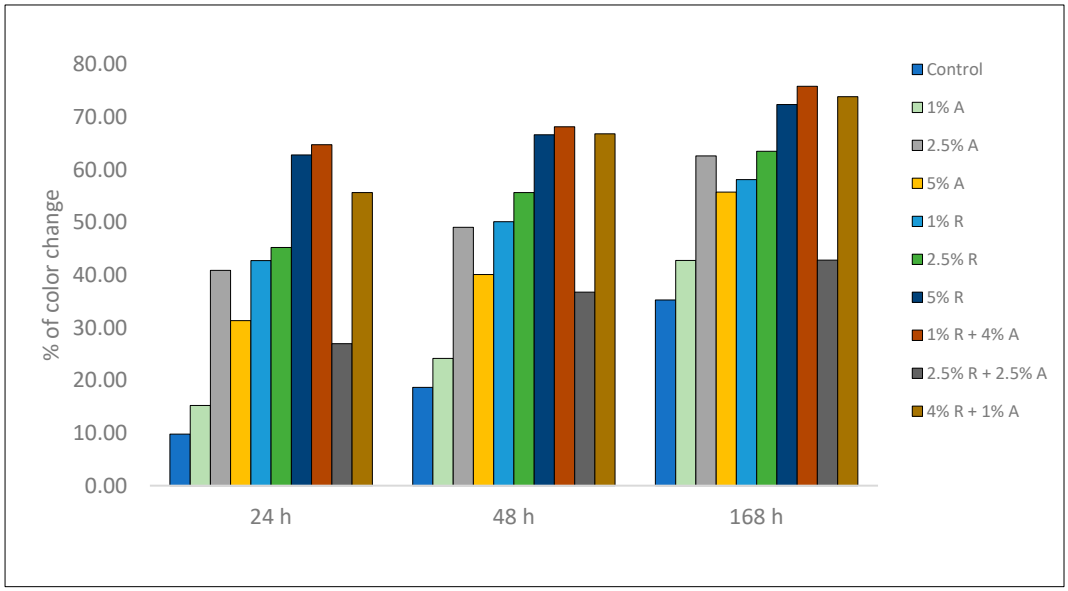


Figure 7. Experimental results for degrading rhodamine B after 24 h, 48 h, and 168 h (7 days).

The results show a significant improvement in the self-cleaning performance of lightweight concrete modified with TiO_2 nanophase, compared with a control sample without the addition of TiO_2. An overall increase in discoloration values was observed for all the tested samples, including the control sample. It should be mentioned that the measured color of the sample surface was strongly dependent on the degree of cement hydration. It was established that the surface color of all the studied materials changed during the hydration process.

Two stages of color change were observed in the rhodamine B, caused by the self-cleaning effect of TiO_2-modified samples. In the first stage, the percentage of color changes in the rhodamine B increased rapidly during the initial 24 h of UV-A irradiation for all samples. The differences in the self-cleaning effect between samples containing anatase, rutile, and anatase-rutile were significant. For the materials named 5 wt % R and 4 wt % A + 1 wt % R, the color change after 24 h of irradiation was the most significant and amounted to over 60%. The control sample and the sample with 1 wt % anatase showed the least noticeable color change, remaining below 15%. The next stage was observed after between 48 h and 168 h of irradiation. The rate at which the color change index increased was slower than for the first stage, resulting in only a slight color alteration. This observation is consistent with the results presented by Liu [82]. Similar to the first stage, the samples that exhibited the smallest color change after 48 h of irradiation were the control sample and the sample with the addition of 1 wt % anatase, while the largest color change (up to 65%) was observed in relation to three samples: 5 wt % R, 4 wt % A + 1 wt % R, and 4 wt % R + 1 wt % A. In the case of UV-A exposure for 168 h, the largest color change was observed in the case of the same samples as

those after 48 h of irradiation, namely, 5 wt % R, 4 wt % A + 1 wt % R, and 4 wt % R + 1 wt % A, wherein the value for the color change exceeded 70%. The obtained data are promising because most of the rhodamine B was removed in the first, active phase of the de-coloration process, which corresponds to the prevention of contaminant agglomeration on the surface.

In the first active stage of the de-coloration of rhodamine B, there was a clearly visible trend of color reduction. Increasing the concentration of rutile from 0 wt % to 5 wt % in TiO_2-modified concrete samples caused an increased degradation of rhodamine B on the surface, due to the photocatalytic reaction. In the case of samples containing anatase, the highest percentage of discoloration was observed for the concrete supplemented with 2.5 wt % of anatase. A similar effect for anatase-modified and rutile-modified samples was noticeable after 48 h and 7 days. Regarding the samples with a 5 wt % addition of TiO_2 for both single-phase samples and a mixture of rutile and anatase, the most significant self-cleaning performance was obtained for the 4 wt % A + 1 wt % R sample (75.85%). The results clearly show the synergistic effect of self-cleaning performance between the two incorporated anatase and rutile phases.

A relatively low degree of discoloration was observed for 2.5 wt % A + 2.5 wt % R samples. This may result from the measurement method being one that does not consider the samples' topography: roughness and porosity. The sample containing an equilibrium mixture of rutile and anatase (2.5 wt %) had the highest open pore content (14.7%) (Figure S1 in the Supplementary Materials).

3.3. Reduction of NO_X

In this paper, the self-cleaning performance of lightweight concrete modified with nanophase TiO_2 was tested. The influence of titanium dioxide concentrations and the ratio of anatase-rutile polymorphs on NO_x reduction was studied. The obtained results are shown in Figure 8.

A significant improvement in the photocatalytic properties of samples modified with titanium dioxide in comparison to the control sample was noted. With an increase in rutile content, the degree of NO_x reduction increases (Figure 9a). The same dependence was not observed in the case of materials containing anatase, while the highest NO_x reduction degree was noted in the case of the sample containing 2.5 wt % of anatase (Figure 9b). These observations are consistent with the results obtained for the analysis of self-cleaning performance, wherein the percentage of discoloration was highest in the sample containing 2.5 wt % of anatase. Taking into account all the studied materials, it must be noted that the best NO_x reduction performance was recorded in the case of the 2.5 wt % A + 2.5 wt % R sample (5.7%). The results of NO_x reduction in samples with the addition of anatase-rutile polymorphs are shown in Figure 9c.

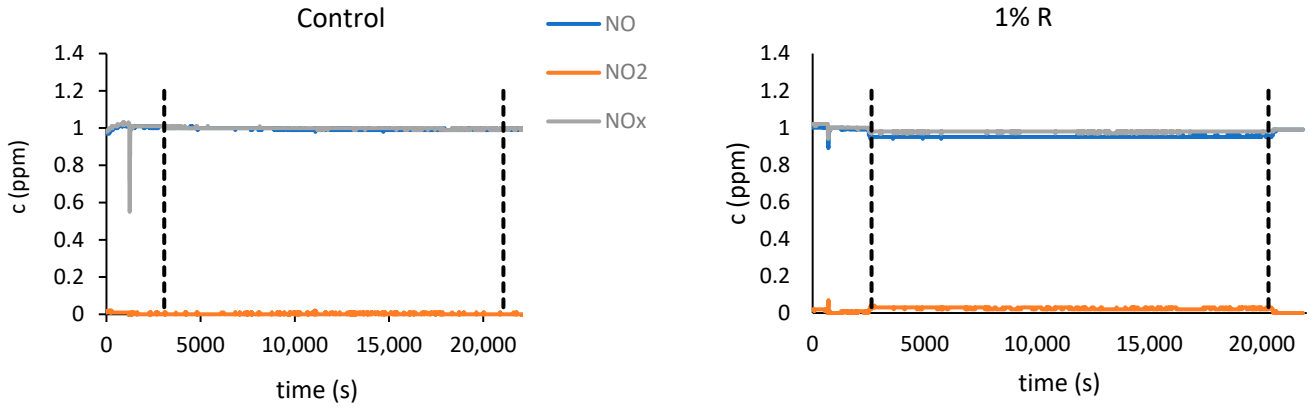


Figure 8. *Cont.*

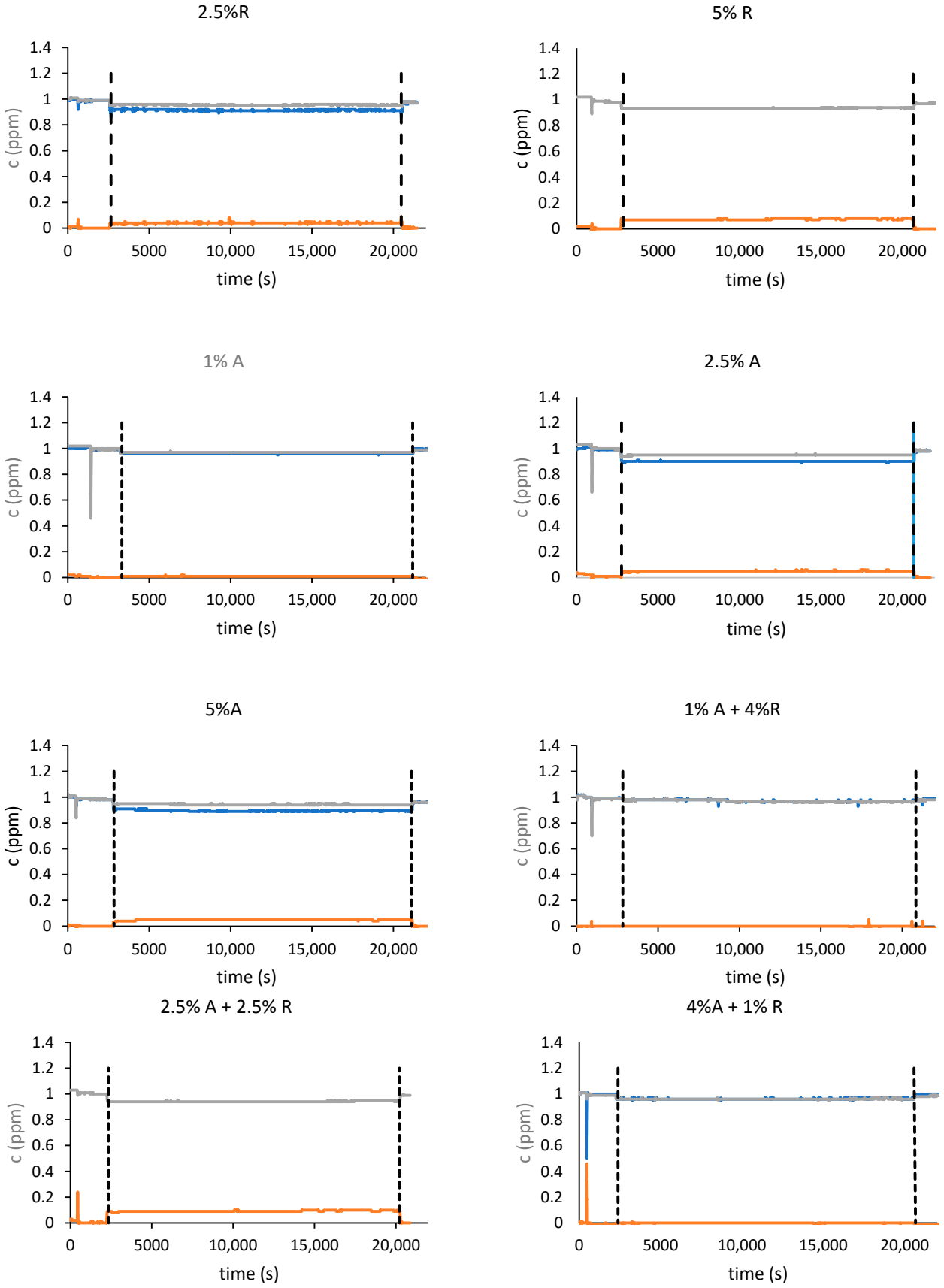
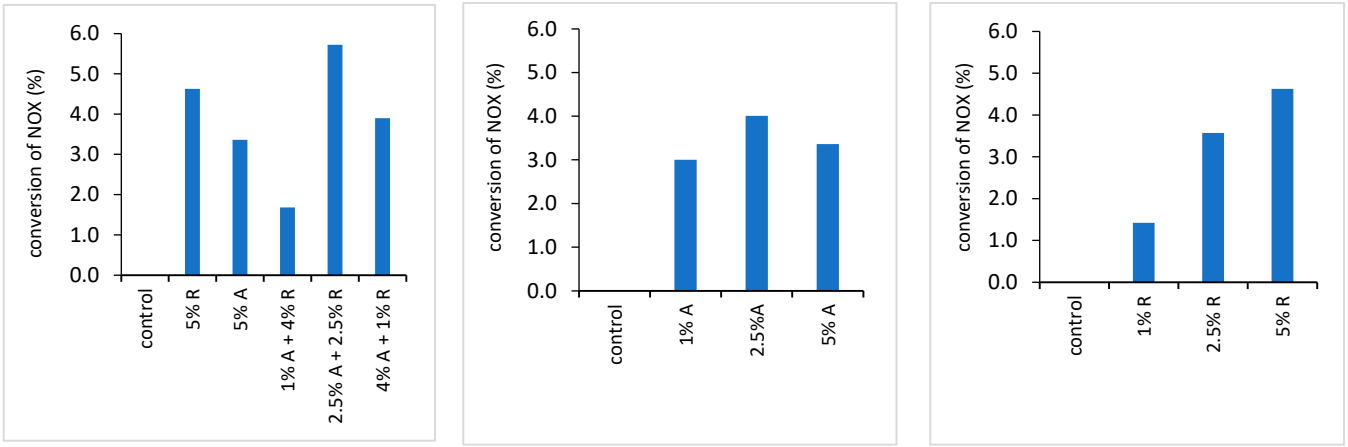


Figure 8. Determination of the photocatalytic activity of lightweight concrete modified with nanophase TiO_2.



(**a**) (**b**) (**c**)

Figure 9. Effectiveness of TiO_2-modified concrete samples in NO_x removal: (**a**) specimens with rutile addition; (**b**) specimens with anatase addition; (**c**) specimens with a 5 wt % addition of TiO_2.

The majority of the authors have noted that anatase has higher photocatalytic activity than rutile [68,69]. However, the results presented in this paper show that the photocatalytic ability regarding self-cleaning and NO_x reduction is better for materials with the addition of rutile. This may be due to the fact that the rutile used in the research was doped with nitrogen. This observation corresponds to the results from Padmanabahan's research [69], which show that the chemical modification of TiO_2 by doping with non-metals such as N can improve the visible light response in TiO_2, thereby driving photocatalysis.

Moreover, the poor NO_x reduction properties observed for 1 wt % of anatase and rutile are in agreement with the results obtained by Folli et al. [83]. The authors noted that satisfactory photocatalytic performance can be achieved using 3–5 wt % of titanium dioxide.

4. Conclusions

In this work, the photocatalytic reduction of NO_x, self-cleaning performance, and antimicrobial properties of nano TiO_2-modified lightweight concrete was studied. Lightweight concrete without the addition of nanometric titanium dioxide, as well as anatase-modified lightweight concrete, rutile-modified lightweight concrete, and anatase-rutile-modified lightweight concrete were tested. Based on the obtained results, the following conclusions can be drawn:

1. The addition of titanium dioxide to lightweight concrete leads to significant improvements in its self-cleaning performance, NO_x reduction, and antimicrobial properties.
2. The photocatalytic ability regarding self-cleaning and NO_x reduction is better in the concrete with the rutile addition compared to the concrete with the anatase addition because the rutile used in this research was doped with nitrogen.
3. The experimental results show a synergistic effect of the polymorphic phases of TiO_2 containing rutile-anatase, but not in every proportion. The best NO_x reduction properties for the equilibrium (2.5 wt %) mixture of anatase and rutile were noted when the sample reached the highest value. These results also correspond to the microbial resistance test results, wherein the best antifungal and anti-algal properties simultaneously were obtained for the 2.5 wt % A + 2.5 wt % R sample. The synergy between the two phases is not well understood; nonetheless, these are very promising results that require further detailed research.
4. The utilization of the combined polymorphs of titanium dioxide in cementitious products can be environmentally beneficial; however, in order to ensure the effective application of such composites, a future comprehensive examination of the mechanical properties of lightweight concrete with the addition of TiO_2 is necessary.

Supplementary Materials: The following supporting information can be downloaded at: https://www.mdpi.com/article/10.3390/buildings13071736/s1, Figure S1: Comparison of the results for the open-pore content of the TiO_2-modified concrete samples.

Author Contributions: Conceptualisation, W.K. and E.O.-K.; software, W.K., A.D.-M. and E.O.-K.; data curation, W.K. and A.D.-M.; writing—original draft preparation, W.K., A.D-M. and E.O.-K.; writing—review and editing, W.K.; E.O.-K. and M.G.; visualization, W.K. and M.G.; supervision, E.O.-K.; project administration, W.K.; A.R. and E.O.-K.; funding acquisition W.K. and E.O.-K. All authors have read and agreed to the published version of the manuscript.

Funding: This research was funded by Nicolaus Copernicus University in Toruń (IDUB, grant INCOOP).

Data Availability Statement: The data presented in this study are available on request from the corresponding author. The data are not publicly available due to project realization.

Conflicts of Interest: The authors declare no conflict of interest.

References

1. Hasan, M.; Saidi, T.; Afifuddin, M. Mechanical Properties and Absorption of Lightweight Concrete Using Lightweight Aggregate from Diatomaceous Earth. *Constr. Build. Mater.* **2021**, *277*, 122324. [CrossRef]
2. Shi, J.; Liu, B.; He, Z.; Liu, Y.; Jiang, J.; Xiong, T.; Shi, J. A Green Ultra-Lightweight Chemically Foamed Concrete for Building Exterior: A Feasibility Study. *J. Clean. Prod.* **2021**, *288*, 125085. [CrossRef]
3. Qiu, L.; Dong, S.; Ashour, A.; Han, B. Antimicrobial Concrete for Smart and Durable Infrastructures: A Review. *Constr. Build. Mater.* **2020**, *260*, 120456. [CrossRef] [PubMed]
4. Wang, X.; Ding, H.; Lv, G.; Zhou, R.; Ma, R.; Hou, X.; Zhang, J.; Li, W. Fabrication of Superhydrophilic Self-Cleaning SiO_2–TiO_2 Coating and Its Photocatalytic Performance. *Ceram. Int.* **2022**, *48*, 20033–20040. [CrossRef]
5. Klapiszewska, I.; Parus, A.; Ławniczak, Ł.; Jesionowski, T.; Klapiszewski, Ł.; Ślosarczyk, A. Production of Antibacterial Cement Composites Containing ZnO/Lignin and ZnO–SiO_2/Lignin Hybrid Admixtures. *Cem. Concr. Compos.* **2021**, *124*, 104250. [CrossRef]
6. Martinez, T.; Bertron, A.; Escadeillas, G.; Ringot, E. Algal Growth Inhibition on Cement Mortar: Efficiency of Water Repellent and Photocatalytic Treatments under UV/VIS Illumination. *Int. Biodeterior. Biodegrad.* **2014**, *89*, 115–1125. [CrossRef]
7. Giannantonio, D.J.; Kurth, J.C.; Kurtis, K.E.; Sobecky, P.A. Effects of Concrete Properties and Nutrients on Fungal Colonization and Fouling. *Int. Biodeterior. Biodegrad.* **2009**, *63*, 252–259. [CrossRef]
8. Dubosc, A.; Escadeillas, G.; Blanc, P.J. Characterization of Biological Stains on External Concrete Walls and Influence of Concrete as Underlying Material. *Cem. Concr. Res.* **2001**, *31*, 1613–1617. [CrossRef]
9. Warscheid, T.; Braams, J. Biodeterioration of Stone: A Review. *Int. Biodeterior. Biodegrad.* **2000**, *46*, 343–368. [CrossRef]
10. Utsev, T.; Tiza, T.M.; Mogbo, O.; Kumar Singh, S.; Chakravarti, A.; Shaik, N.; Pal Singh, S. Application of Nanomaterials in Civil Engineering. *Mater. Today Proc.* **2022**, *62*, 5140–5146. [CrossRef]
11. Akarsh, P.K.; Shrinidhi, D.; Marathe, S.; Bhat, A.K. Graphene Oxide as Nano-Material in Developing Sustainable Concrete—A Brief Review. *Mater. Today Proc.* **2022**, *60*, 234–246. [CrossRef]
12. Luna, M.; Delgado, J.J.; Romero, I.; Montini, T.; Almoraima Gil, M.L.; Martínez-López, J.; Fornasiero, P.; Mosquera, M.J. Photocatalytic TiO_2 Nanosheets-SiO_2 Coatings on Concrete and Limestone: An Enhancement of de-Polluting and Self-Cleaning Properties by Nanoparticle Design. *Constr. Build. Mater.* **2022**, *338*, 127349. [CrossRef]
13. Bica, B.O.; de Melo, J.V.S. Concrete Blocks Nano-Modified with Zinc Oxide (ZnO) for Photocatalytic Paving: Performance Comparison with Titanium Dioxide (TiO_2). *Constr. Build. Mater.* **2020**, *252*, 119120. [CrossRef]
14. Shen, W.; Zhang, C.; Li, Q.; Zhang, W.; Cao, L.; Ye, J. Preparation of Titanium Dioxide Nano Particle Modified Photocatalytic Self-Cleaning Concrete. *J. Clean. Prod.* **2015**, *87*, 762–765. [CrossRef]
15. Ortega-Villar, R.; Lizárraga-Mendiola, L.; Coronel-Olivares, C.; López-León, L.D.; Bigurra-Alzati, C.A.; Vázquez-Rodríguez, G.A. Effect of Photocatalytic Fe2O3 Nanoparticles on Urban Runoff Pollutant Removal by Permeable Concrete. *J. Environ. Manag.* **2019**, *242*, 487–495. [CrossRef]
16. Chekravarty, D.S.V.S.M.R.K.; Alapati, M.; Sravana, P.; Srinivasa Rao, P. Experimental Investigations on Durability Properties Nano-Silica Based Concrete. *Mater. Today Proc.* **2022**, *51*, 2176–2184. [CrossRef]
17. Saleh, A.N.; Attar, A.A.; Ahmed, O.K.; Mustafa, S.S. Improving the Thermal Insulation and Mechanical Properties of Concrete Using Nano-SiO_2. *Results Eng.* **2021**, *12*, 100303. [CrossRef]
18. Krishnaveni, C.; Senthil Selvan, S. Study on Nano-Alumina in Concrete. *Mater. Today Proc.* **2021**, *46*, 3648–3652. [CrossRef]
19. Sargunan, K.; Venkata Rao, M.; Alex Rajesh, A.; Babu, R.; Prasanthni, P.; Jagadeep, K.; Rinawa, M.L. Experimental Investigations on Mechanical Strength of Concrete Using Nano-Alumina and Nano-Clay. *Mater. Today Proc.* **2022**, *62*, 5420–5426. [CrossRef]
20. Tufail, R.F.; Naeem, M.H.; Ahmad, J.; Waheed, H.; Majdi, A.; Farooq, D.; Maqsoom, A.; Butt, F. Evaluation of the Fresh and Mechanical Properties of Nano-Engineered Self Compacting Concrete Containing Graphite Nano/Micro Platelets. *Case Stud. Constr. Mater.* **2022**, *17*, e01165. [CrossRef]

21. Mudasir, P.; Naqash, J.A. Impact of Carbon Nano Tubes on Fresh and Hardned Properties of Conventional Concrete. *Mater. Today Proc.* **2021**, *80*, 1920–1925. [CrossRef]
22. Ren, J.; Luo, X.; Bai, R.; Pan, C.; Zhang, J. Pore Characteristics of Different Phase in Nano-Modified Concrete and Their Influences on the Compressive Strength. *J. Build. Eng.* **2022**, *46*, 103784. [CrossRef]
23. Amor, F.; Baudys, M.; Racova, Z.; Scheinherrová, L.; Ingrisova, L.; Hajek, P. Contribution of TiO_2 and ZnO Nanoparticles to the Hydration of Portland Cement and Photocatalytic Properties of High Performance Concrete. *Case Stud. Constr. Mater.* **2022**, *16*, e00965. [CrossRef]
24. Ballari, M.M.; Hunger, M.; Hüsken, G.; Brouwers, H.J.H. NO_x Photocatalytic Degradation Employing Concrete Pavement Containing Titanium Dioxide. *Appl. Catal. B* **2010**, *95*, 245–254. [CrossRef]
25. Ruot, B.; Plassais, A.; Olive, F.; Guillot, L.; Bonafous, L. TiO_2-Containing Cement Pastes and Mortars: Measurements of the Photocatalytic Efficiency Using a Rhodamine B-Based Colourimetric Test. *Sol. Energy* **2009**, *83*, 1794–1801. [CrossRef]
26. Dong, W.; Huang, Y.; Lehane, B.; Aslani, F.; Ma, G. Mechanical and Electrical Properties of Concrete Incorporating an Iron-Particle Contained Nano-Graphite by-Product. *Constr. Build. Mater.* **2021**, *270*, 121377. [CrossRef]
27. Zhang, G.; Chen, L.; Fu, X.; Wang, H. Cellulose Microfiber-Supported TiO_2@Ag Nanocomposites: A Dual-Functional Platform for Photocatalysis and in Situ Reaction Monitoring. *Ind. Eng. Chem. Res.* **2018**, *57*, 4277–4286. [CrossRef]
28. Zhang, J.; Liu, Z. Fabrication and Characterization of Eu 2+ -Doped Lanthanum-Magnesium-Gallium /TiO_2 -Based Composition as Photocatalytic Materials for Cement Concrete-Related Methyl Orange (MO) Degradation. *Ceram. Int.* **2019**, *45*, 10342–10347. [CrossRef]
29. Worasawat, S.; Tasaki, K.; Hatanaka, Y.; Neo, Y.; Mimura, H.; Pecharapa, W. Growth of ZnO Nano-Rods and Its Photoconductive Characteristics on the Photo-Catalytic Properties. *Mater. Today Proc.* **2019**, *17*, 1379–1385. [CrossRef]
30. Hanaor, D.A.H.; Sorrell, C.C. Review of the Anatase to Rutile Phase Transformation. *J. Mater. Sci.* **2011**, *46*, 855–874. [CrossRef]
31. Zhang, J.; Zhou, P.; Liu, J.; Yu, J. New Understanding of the Difference of Photocatalytic Activity among Anatase, Rutile and Brookite TiO_2. *Phys. Chem. Chem. Phys.* **2014**, *16*, 20382–20386. [CrossRef] [PubMed]
32. Guo, M.Z.; Ling, T.C.; Poon, C.S. Nano-TiO_2-Based Architectural Mortar for NO Removal and Bacteria Inactivation: Influence of Coating and Weathering Conditions. *Cem. Concr. Compos.* **2013**, *36*, 101–108. [CrossRef]
33. Jin, Q.; Saad, E.M.; Zhang, W.; Tang, Y.; Kurtis, K.E. Quantification of NO_x Uptake in Plain and TiO_2-Doped Cementitious Materials. *Cem. Concr. Res.* **2019**, *122*, 251–256. [CrossRef]
34. Kim, H.J.; Yoon, Y.S.; Yang, K.H.; Kwon, S.J. Durability and Purification Performance of Concrete Impregnated with Silicate and Sprayed with Photocatalytic TiO_2. *Constr. Build. Mater.* **2019**, *199*, 106–114. [CrossRef]
35. Maury-Ramirez, A.; Demeestere, K.; De Belie, N. Photocatalytic Activity of Titanium Dioxide Nanoparticle Coatings Applied on Autoclaved Aerated Concrete: Effect of Weathering on Coating Physical Characteristics and Gaseous Toluene Removal. *J. Hazard. Mater.* **2012**, *211–212*, 218–225. [CrossRef]
36. Cardellicchio, L. Self-Cleaning and Colour-Preserving Efficiency of Photocatalytic Concrete: Case Study of the Jubilee Church in Rome. *Build. Res. Inf.* **2020**, *48*, 160–179. [CrossRef]
37. Diamanti, M.V.; Del Curto, B.; Ormellese, M.; Pedeferri, M.P. Photocatalytic and Self-Cleaning Activity of Colored Mortars Containing TiO_2. *Constr. Build. Mater.* **2013**, *46*, 167–174. [CrossRef]
38. Wang, Z.; Yu, Q.; Feng, P.; Brouwers, H.J.H. Variation of Self-Cleaning Performance of Nano-TiO_2 Modified Mortar Caused by Carbonation: From Hydrates to Carbonates. *Cem. Concr. Res.* **2022**, *158*, 106852. [CrossRef]
39. Pacheco-Torgal, F.; Jalali, S. Cementitious Building Materials Reinforced with Vegetable Fibres: A Review. *Constr. Build. Mater.* **2011**, *25*, 575–581. [CrossRef]
40. Ekincioglu, O.; Özkul, M.H.; Patachia, S.; Moise, G. Effect of TiO_2 Addition on the Properties of Macro Defect Free Cement-Polymer Composites. *Restor. Build. Monum.* **2013**, *19*, 125–134. [CrossRef]
41. Jamal, P. Immobilization of TiO_2 with Cement: Photocatalytic Degradation of Phenol and Its Kinetic Studies. *Artic. Indian J. Chem. Technol.* **2011**, *18*, 263–270.
42. Nazari, A.; Riahi, S. The Effects of TiO_2 Nanoparticles on Properties of Binary Blended Concrete. *J. Compos. Mater.* **2011**, *45*, 1181–1188. [CrossRef]
43. Lucas, S.S.; Ferreira, V.M.; De Aguiar, J.L.B. Incorporation of Titanium Dioxide Nanoparticles in Mortars—Influence of Microstructure in the Hardened State Properties and Photocatalytic Activity. *Cem. Concr. Res.* **2013**, *43*, 112–120. [CrossRef]
44. Diamanti, M.V.; Ormellese, M.; Pedeferri, M.P. Characterization of Photocatalytic and Superhydrophilic Properties of Mortars Containing Titanium Dioxide. *Cem. Concr. Res.* **2008**, *38*, 1349–1353. [CrossRef]
45. Vittoriadiamanti, M.; Pedeferri, M.P. Concrete, Mortar and Plaster Using Titanium Dioxide Nanoparticles: Applications in Pollution Control, Self-Cleaning and Photo Sterilization. In *Nanotechnology in Eco-Efficient Construction: Materials, Processes and Applications*; Woodhead Publishing: Soston, UK, 2013; pp. 299–326. [CrossRef]
46. Janus, M.; Zatorska, J.; Czyzewski, A.; Bubacz, K.; Kusiak-Nejman, E.; Morawski, A.W. Self-Cleaning Properties of Cement Plates Loaded with N,C-Modified TiO_2 Photocatalysts. *Appl. Surf. Sci.* **2015**, *330*, 200–206. [CrossRef]
47. Huang, Z.; Maness, P.-C.; Blake, D.M.; Wolfrum, E.J.; Smolinski, S.L.; Jacoby, W.A. Bactericidal Mode of Titanium Dioxide Photocatalysis. *J. Photochem. Photobiol. A Chem.* **2000**, *130*, 163–170. [CrossRef]
48. Sunada, K.; Watanabe, T.; Hashimoto, K. Studies on Photokilling of Bacteria on TiO_2 Thin Film. *J. Photochem. Photobiol. A Chem.* **2003**, *156*, 227–233. [CrossRef]

49. Maury-Ramirez, A.; De Muynck, W.; Stevens, R.; Demeestere, K.; De Belie, N. Titanium Dioxide Based Strategies to Prevent Algal Fouling on Cementitious Materials. *Cem. Concr. Compos.* **2013**, *36*, 93–100. [CrossRef]
50. Allen, N.S.; Edge, M.; Verran, J.; Stratton, J.; Maltby, J.; Bygott, C. Photocatalytic Titania Based Surfaces: Environmental Benefits. *Polym. Degrad. Stab.* **2008**, *93*, 1632–1646. [CrossRef]
51. Janus, M.; Kusiak-Nejman, E.; Rokicka-Konieczna, P.; Markowska-Szczupak, A.; Zając, K.; Morawski, A.W. Bacterial Inactivation on Concrete Plates Loaded with Modified TiO_2 Photocatalysts under Visible Light Irradiation. *Molecules* **2019**, *24*, 3026. [CrossRef]
52. Ganji, N.; Allahverdi, A.; Naeimpoor, F.; Mahinroosta, M. Photocatalytic Effect of Nano-TiO_2 Loaded Cement on Dye Decolorization and Escherichia Coli Inactivation under UV Irradiation. *Res. Chem. Intermed.* **2016**, *42*, 5395–5412. [CrossRef]
53. Fonseca, A.J.; Pina, F.; Macedo, M.F.; Leal, N.; Romanowska-Deskins, A.; Laiz, L.; Gómez-Bolea, A.; Saiz-Jimenez, C. Anatase as an Alternative Application for Preventing Biodeterioration of Mortars: Evaluation and Comparison with Other Biocides. *Int. Biodeterior. Biodegrad.* **2010**, *64*, 388–396. [CrossRef]
54. Linkous, C.A.; Carter, G.J.; Locuson, D.B.; Ouellette, A.J.; Slattery, D.K.; Smitha, L.A. Photocatalytic Inhibition of Algae Growth Using TiO_2, WO3, and Cocatalyst Modifications. *Environ. Sci. Technol.* **2000**, *34*, 4754–4758. [CrossRef]
55. Tuntachon, S.; Kamwilaisak, K.; Somdee, T.; Mongkoltanaruk, W.; Sata, V.; Boonserm, K.; Wongsa, A.; Chindaprasirt, P. Resistance to Algae and Fungi Formation of High Calcium Fly Ash Geopolymer Paste Containing TiO_2. *J. Build. Eng.* **2019**, *25*, 100817. [CrossRef]
56. Harilal, M.; Anandkumar, B.; Lahiri, B.B.; George, R.P.; Philip, J.; Albert, S.K. Enhanced Biodeterioration and Biofouling Resistance of Nanoparticles and Inhibitor Admixed Fly Ash Based Concrete in Marine Environments. *Int. Biodeterior. Biodegrad.* **2020**, *155*, 105088. [CrossRef]
57. Nath, R.K.; Zain, M.F.M.; Jamil, M. An Environment-Friendly Solution for Indoor Air Purification by Using Renewable Photocatalysts in Concrete: A Review. *Renew. Sustain. Energy Rev.* **2016**, *62*, 1184–1194. [CrossRef]
58. Cowan, A.J.; Durrant, J.R. Long-Lived Charge Separated States in Nanostructured Semiconductor Photoelectrodes for the Production of Solar Fuels. *Chem. Soc. Rev.* **2013**, *42*, 2281–2293. [CrossRef]
59. Yang, L.; Hakki, A.; Zheng, L.; Jones, M.R.; Wang, F.; Macphee, D.E. Photocatalytic Concrete for NO_x Abatement: Supported TiO_2 Efficiencies and Impacts. *Cem. Concr. Res.* **2019**, *116*, 57–64. [CrossRef]
60. MacPhee, D.E.; Folli, A. Photocatalytic Concretes—The Interface between Photocatalysis and Cement Chemistry. *Cem. Concr. Res.* **2016**, *85*, 48–54. [CrossRef]
61. Sujatha, G.; Shanthakumar, S.; Chiampo, F. UV Light-irradiated Photocatalytic Degradation of Coffee Processing Wastewater Using TiO_2 as a Catalyst. *Environments* **2020**, *7*, 47. [CrossRef]
62. Fiore, A.; Marano, G.C.; Monaco, P.; Morbi, A. Preliminary Experimental Study on the Effects of Surface-Applied Photocatalytic Products on the Durability of Reinforced Concrete. *Constr. Build. Mater.* **2013**, *48*, 137–143. [CrossRef]
63. Hüsken, G.; Hunger, M.; Brouwers, H.J.H. Experimental Study of Photocatalytic Concrete Products for Air Purification. *Build. Environ.* **2009**, *44*, 2463–2474. [CrossRef]
64. *EN 196-1:2016*; Methods of Testing Cement—Part 1: Determination of Strength. British Standards Institution: London, UK, 2016.
65. *ISO 22197-1*; Fine Ceramics (Advanced Ceramics, Advanced Technical Ceramics). Test Method for Air-Purification Performance of Semiconducting Photocatalytic Materials. Part 1: Removal of Nitric Oxide. ISO: Geneva, Switzerland, 2016.
66. George, R.P.; Ramya, S.; Ramachandran, D.; Kamachi Mudali, U. Studies on Biodegradation of Normal Concrete Surfaces by Fungus *Fusarium* Sp. *Cem. Concr. Res.* **2013**, *47*, 8–13. [CrossRef]
67. Czaczyk, K.; Biotechnologii, K.; Żywności, M.; Wojciechowska, K. Tworzenie Biofllmów Bakteryjnych Istota Zjawiska i Mechanizmy Oddziaływań. *Biotechnologia* **2003**, *3*, 180–192.
68. Nikoomanzari, E.; Karbasi, M.; Melo, W.C.; Moris, H.; Babaei, K.; Giannakis, S.; Fattah-alhosseini, A. Impressive Strides in Antibacterial Performance Amelioration of Ti-Based Implants via Plasma Electrolytic Oxidation (PEO): A Review of the Recent Advancements. *Chem. Eng. J.* **2022**, *441*, 136003. [CrossRef]
69. Padmanabhan, N.T.; John, H. Titanium Dioxide Based Self-Cleaning Smart Surfaces: A Short Review. *J. Environ. Chem. Eng.* **2020**, *8*, 104211. [CrossRef]
70. Matsunaga, T.; Tomoda, R.; Nakajima, T.; Wake, H. Photoelectrochemical Sterilization of Microbial Cells by Semiconductor Powders. *FEMS Microbiol. Lett.* **1985**, *29*, 211–214. [CrossRef]
71. Ribas, S. Study of Biological Degradation Applied to Concrete. In *Transactions of the 13 International Conference on Structural Mechanics in Reactor Technology-SMiRT*; University Federal Do Rio Grande Do Sul: Porto Alegre, Brazil, 1995.
72. Sanchez-Silva, M.; Asce, A.M.; Rosowsky, D.V.; Asce, M. Biodeterioration of Construction Materials: State of the Art and Future Challenges. *J. Mater. Civ. Eng.* **2008**, *20*, 352–365. [CrossRef]
73. Markowska-Szczupak, A.; Wang, K.; Rokicka, P.; Endo, M.; Wei, Z.; Ohtani, B.; Morawski, A.W.; Kowalska, E. The Effect of Anatase and Rutile Crystallites Isolated from Titania P25 Photocatalyst on Growth of Selected Mould Fungi. *J. Photochem. Photobiol. B* **2015**, *151*, 54–62. [CrossRef]
74. Yu, J.; Yu, J.C.; Leung, M.K.P.; Ho, W.; Cheng, B.; Zhao, X.; Zhao, J. Effects of Acidic and Basic Hydrolysis Catalysts on the Photocatalytic Activity and Microstructures of Bimodal Mesoporous Titania. *J. Catal.* **2003**, *217*, 69–78. [CrossRef]
75. Hou, J.; Wang, L.; Wang, C.; Zhang, S.; Liu, H.; Li, S.; Wang, X. Toxicity and Mechanisms of Action of Titanium Dioxide Nanoparticles in Living Organisms. *J. Environ. Sci.* **2019**, *75*, 40–53. [CrossRef] [PubMed]

76. Reddy, P.V.L.; Kavitha, B.; Reddy, P.A.K.; Kim, K.-H. TiO_2-based photocatalytic disinfection of microbes in aqueous media: A review. *Environ. Res.* **2017**, *154*, 296–303. [CrossRef] [PubMed]
77. Krumdieck, S.P.; Boichot, R.; Gorthy, R.; Land, J.G.; Lay, S.; Gardecka, A.J.; Polson, M.I.J.; Wasa, A.; Aitken, J.E.; Heinemann, J.A.; et al. Nanostructured TiO_2 Anatase-Rutile-Carbon Solid Coating with Visible Light Antimicrobial Activity. *Sci. Rep.* **2019**, *9*, 1883. [CrossRef] [PubMed]
78. Werle, A.P.; De Souza, M.L.; Loh, K.; Ando, R.; John, V.M. The Performance of a Self-Cleaning Cool Cementitious Surface. *Energy Build.* **2016**, *114*, 200–205. [CrossRef]
79. Zhao, A.; Yang, J.; Yang, E.H. Self-Cleaning Engineered Cementitious Composites. *Cem Concr Compos* **2015**, *64*, 74–83. [CrossRef]
80. Diamanti, M.V.; Paolini, R.; Rossini, M.; Aslan, A.B.; Zinzi, M.; Poli, T.; Pedeferri, M.P. Long Term Self-Cleaning and Photocatalytic Performance of Anatase Added Mortars Exposed to the Urban Environment. *Constr. Build. Mater.* **2015**, *96*, 270–278. [CrossRef]
81. Khataee, R.; Heydari, V.; Moradkhannejhad, L.; Safarpour, M.; Joo, S.W. Self-Cleaning and Mechanical Properties of Modified White Cement with Nanostructured TiO_2. *J. Nanosci. Nanotechnol.* **2013**, *13*, 5109–5114. [CrossRef]
82. Liu, D.; Kaja, A.; Chen, Y.; Brouwers, H.J.H.; Yu, Q. Self-Cleaning Performance of Photocatalytic Cement Mortar: Synergistic Effects of Hydration and Carbonation. *Cem. Concr. Res.* **2022**, *162*, 107009. [CrossRef]
83. Folli, A.; Pade, C.; Hansen, T.B.; De Marco, T.; MacPhee, D.E. TiO_2 Photocatalysis in Cementitious Systems: Insights into Self-Cleaning and Depollution Chemistry. *Cem. Concr. Res.* **2012**, *42*, 539–548. [CrossRef]

Disclaimer/Publisher's Note: The statements, opinions and data contained in all publications are solely those of the individual author(s) and contributor(s) and not of MDPI and/or the editor(s). MDPI and/or the editor(s) disclaim responsibility for any injury to people or property resulting from any ideas, methods, instructions or products referred to in the content.